# Uniform Si-CHA Zeolite Layers Formed by a Selective Sonication-Assisted Deposition Method**

*Eunjoo Kim, Wanxi Cai, Hionsuck Baik, and Jungkyu Choi*

Zeolites are crystalline aluminosilicate materials employed in a wide range of applications, including catalysis, separation, water softening, and adsorption.[1–4] The rigid molecular-sized pores within zeolites are desirable for use in separations because they enable the discrimination and separation of gas molecules on the basis of their size and/or shape.[5–10] This intrinsic molecular-sifting property also holds promise for the selective isolation of $CO_2$ from mixtures, for example, the $CO_2/N_2/H_2O$ mixture that results from postcombustion processes[11–13] and the $CO_2/CH_4/H_2O$ mixture in the natural-gas stream.[14,15] Zeolite pore sizes corresponding to eight-membered rings (8-MRs) lie in the range suitable for $CO_2$ separation, as they are a little larger than $CO_2$ and smaller than or similar in size to $N_2$ or $CH_4$. Specifically, the kinetic diameters of $CO_2$, $N_2$, and $CH_4$ are 0.33, 0.364, and 0.38 nm, respectively, whereas the maximum free dimension of 8-MRs is about 0.43 nm.[2] Multiple 8-MR zeolite membranes have been fabricated in an attempt to capture $CO_2$ from mixtures.[16–21] Specifically, 8-MR zeolite and zeolite-like membranes, such as DDR (decadodecasil 3R)[17,18,22] and SAPO-34 (CHA type, but comprised of silicon, aluminum, phosphate, and oxygen)[16,19,20,23] membranes, respectively, have exhibited high performance for $CO_2$ separation. The pore apertures of pure-silica CHA-type zeolites (Si-CHA zeolites) are about $0.370 \times 0.417$ nm$^2$,[24] which enables the discrimination of $CO_2$ and $N_2$ according to their size. Although the separation of $CO_2$ from $N_2$ is possible by size exclusion with 8-MR pore apertures, the separation of $CO_2$ from $H_2O$ is more challenging owing to the smaller molecular size of $H_2O$ (0.265 nm).[2] To minimize $H_2O$ flux through CHA membranes, their hydrophilicity, which is presumably due to Al constituents in the CHA framework, should be minimized by the use of an all-silica CHA zeolite.

Despite the high potential for $CO_2$ separation even in the presence of $H_2O$, to the best of our knowledge, all-silica CHA (Si-CHA) zeolite membranes have not yet been reported. In particular, the uniform formation of a layer (often called a seed layer) in the secondary growth method is important for the formation of continuous Si-CHA films through subsequent hydrothermal growth.[25–27] However, the synthesis of submicrometer-sized and monodispersed Si-CHA zeolite particles is challenging.[28] Thus, the formation of uniform layers and in turn continuous films by secondary growth is hindered. The difficulties associated with the synthesis can be attributed to the inhomogeneous environment in a solidlike precursor in fluoride media: until now accepted conditions for the effective synthesis of Si-CHA zeolites.[28] Furthermore, a preferential out-of-plane orientation in the seed layer is critical for the manufacture of films with the same orientation and often improves their separation performance by providing desired pore channels perpendicular to the film surface.[27,29]

In this study, we attempted to construct uniform, oriented Si-CHA deposits that could serve as good seed layers. First, we synthesized Si-CHA particles by the conventional synthetic protocol reported by Camblor and co-workers.[28] As reported, near-cubic Si-CHA particles were observed as the dominant product,[24,30–32] although platelike Si-CHA particles were also detected as a minor product. The consideration that the shortest dimension perpendicular to the large basal plane in platelike Si-CHA particles would be beneficial in the formation of an oriented layer led us to develop a method for depositing only the platelike Si-CHA particles on a porous α-$Al_2O_3$ disk. This goal would be quite challenging with conventional coating methods (e.g., dip coating, spin coating). Despite their relatively low abundance, platelike Si-CHA particles were deposited selectively onto the α-$Al_2O_3$ disk by a sonication-assisted method with the successful formation of uniform *h0h*-out-of-plane-oriented layers. To avoid any undesired effect, we calcined all the samples in the form of particles, layers, and films in this study.

Figure 1a,b shows SEM images of particles synthesized with composition t (10 $SiO_2$/5 *N,N,N*-trimethyl-1-adamant-ammonium hydroxide (TMAdaOH)/5 HF/30 $H_2O$) at 155 °C for 42 h. Near-cubic particles (the conventional morphology of Si-CHA zeolites) were easily observed in a wide size distribution of about 1–10 μm. The Bravais–Friedel–Donnay–Harker (BFDH) method suggests that the face of the near-cubic particles is a (101) plane (inset in Figure 1a; see also Scheme S1 in the Supporting Information). To the best of our knowledge, only Si-CHA particles with a near-cubic morphology have been reported previously.[24,30–32] However, as a minor product, we found platelike particles (indicated by

[*] E. Kim, W. Cai, Prof. J. Choi
Department of Chemical and Biological Engineering
College of Engineering, Korea University
Anam-Dong, Seongbuk-Gu, Seoul 136-713 (Republic of Korea)
E-mail: jungkyu_choi@korea.ac.kr

Dr. H. Baik
Korea Basic Science Institute, Seoul Center
Anam-Dong, Seongbuk-Gu, Seoul 136-713 (Republic of Korea)

Supporting information for this article is available on the WWW under http://dx.doi.org/10.1002/anie.201301265.
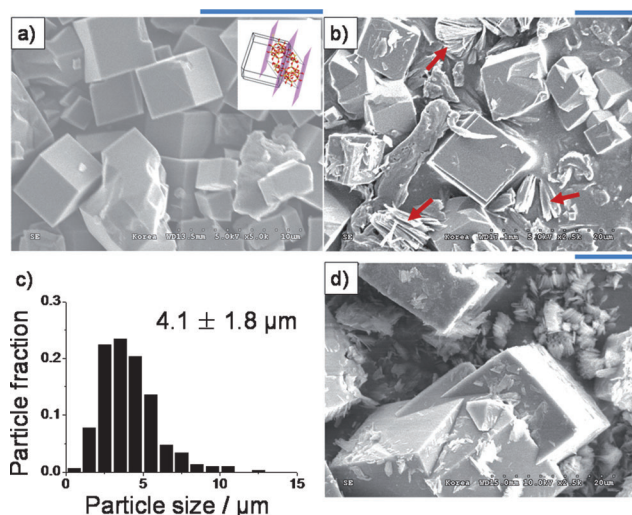
© 2013 Wiley-VCH Verlag GmbH & Co. KGaA, Weinheim

**Figure 1.** a,b) SEM images of particles synthesized with composition t at 155 °C for 42 h and c) the corresponding particle-size distribution of the near-cubic particles. d) SEM image of particles synthesized with composition T at 155 °C for 64 h. The inset in (a) shows the near-cubic particle generated by the BFDH method with Materials Studio (version 5.5). The face of the near-cubic particles (violet) denotes the (101) planes. Brown arrows in (b) indicate platelike particles. Scale bars above the SEM images: 10 μm.



**Figure 2.** a) Simulated XRD pattern of a CHA zeolite. b,c) XRD patterns of as-synthesized particles. The simulated XRD pattern of as-synthesized Si-CHA zeolite powder was generated with the Mercury software (Cambridge Crystallographic Data Centre, CCDC), and the corresponding crystal-information file (#201658) reported by Morris and co-workers[33] was downloaded via "Request a Structure" on the CCDC website (http://www.ccdc.cam.ac.uk).

arrows in Figure 1b), which were often observed in an aggregated form. It appears that under the synthetic conditions of composition t, the platelike particles were synthesized concomitantly with the major product: the near-cubic particles. Figure 1c shows that the near-cubic particles had a wide particle-size distribution, in analogy with the findings of previous studies.[24,30–32] The average particle size and the corresponding standard deviation were approximately 4.1 and 1.8 μm, respectively. Figure 1d shows particles synthesized with composition T, in which the molar ratio of $H_2O$ to $SiO_2$ was changed from about 3:1 (in composition t) to about 1:1. Platelike particles of submicrometer thickness were observed along with near-cubic particles (still the major product). This result possibly indicates that the locally reduced water content in composition T is more favorable for the formation of Si-CHA particles with a platelike morphology.

Figure 2 shows XRD patterns of the as-synthesized particles shown in Figure 1 along with the simulated powder XRD pattern.[33] The XRD patterns indicated that all particles shown in Figure 1 were pure CHA zeolites. Owing to the near-solid nature of the synthetic precursor, it is possible that the molar composition was inhomogeneous during the reaction. Although we attempted to homogenize the near-solid precursor through intensive hand grinding prior to the reaction, the molar composition of the reactants, especially the $H_2O/SiO_2$ ratio, may still have been locally heterogeneous. Thus, the 3:1 molar ratio of $H_2O$ to $SiO_2$ in composition t was probably decreased locally, and the decreased ratio promoted the formation of Si-CHA zeolites with a platelike morphology, as supported by the presence of platelike particles in the product synthesized with composition T (Figure 1d).
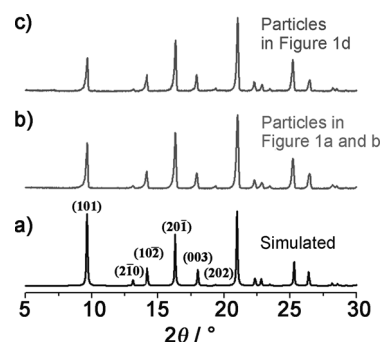
The SEM images in Figure 1 demonstrate the coexistence of platelike particles alongside near-cubic particles as a minor fraction of the mixture. The XRD patterns in Figure 2 confirm the pure CHA crystal phase of the particles in Figure 1. However, the XRD patterns could be dominated by the more abundant near-cubic Si-CHA particles. Therefore, we attempted to isolate the platelike particles from the larger near-cubic particles on the basis of the hypothesis that the latter would precipitate more quickly than the former. The resulting XRD patterns for particles synthesized with composition t confirmed that the recovered particles predominantly consisted of a CHA zeolite phase, although SEM characterization indicated that some near-cubic particles still remained (see Figure S1a,b in the Supporting Information). A minor fraction of amorphous particles was also observed (indicated by arrows in Figure S1b). In contrast, SEM images of particles recovered by applying the above-mentioned precipitation method to the particles synthesized with composition T showed that more platelike Si-CHA particles were produced (see Figure S1c,d).

We subsequently adopted a more selective method for the characterization of the platelike particles. Figure 3a shows a TEM image of a platelike particle next to a near-cubic particle. A selected-area electron-diffraction (SAED) pattern obtained for the marked region in Figure 3a indicated that the platelike particle was the pure CHA zeolite (Figure 3b). Indexing of the spots revealed that the zone axis corresponding to the SAED pattern was [111]. The corresponding simulated SAED pattern marked in red was identical to the experimental counterpart and thus confirmed the validity of the proposed [111] zone axis. Figure 3c shows a high-resolution (HR) TEM image of the platelike particle shown in Figure 3a. Fast Fourier transform (FFT) of the HR TEM image in Figure 3c produced a spot pattern similar to the SAED pattern in Figure 3b; in this way, we could cross-validate the conclusions made on the basis of SAED and HR TEM analysis. TEM images of additional platelike and near-cubic particles are shown with the corresponding SAED patterns in Figures S2 and S3, respectively. Indexing of the
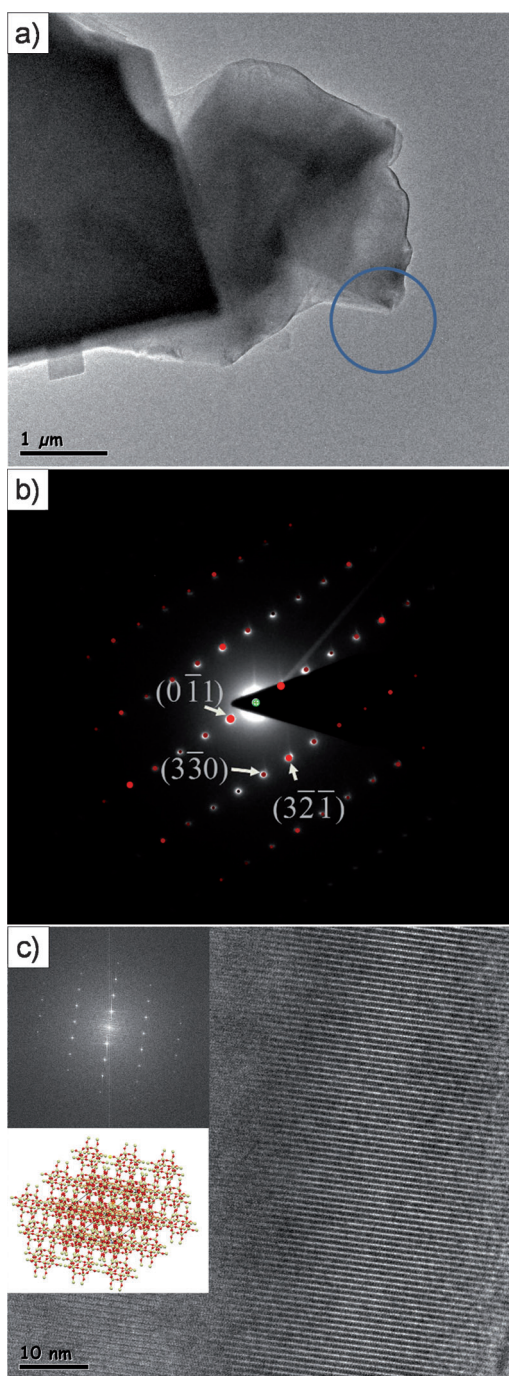
**Figure 3.** a) TEM image, b) SAED pattern, and c) HR TEM image of a platelike particle in Figure 1 b. In (b), the simulated SAED pattern marked in red is superimposed on the experimental counterpart. In (c), the FFT result of the HR TEM image and the structural model projected along the [111] zone axis are shown as insets.
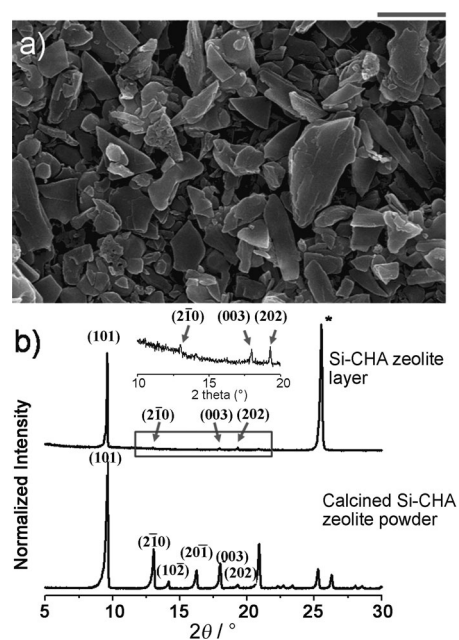


**Figure 4.** a) SEM image of a Si-CHA zeolite layer (scale bar: 1 µm) and b) the corresponding XRD pattern along with the XRD pattern of calcined Si-CHA zeolite powder (the asterisk (*) indicates the peak from the $\alpha$-$Al_2O_3$ disk). The crystallographic preferential orientation (CPO) index was estimated to be approximately $24 \pm 8$ by comparison of the peaks corresponding to the (101) and ($2\bar{1}0$) planes in the XRD patterns of the Si-CHA zeolite particles and the Si-CHA layer.

SAED spots, which were identical to those in the corresponding simulated SAED patterns, supported a [211] zone axis in both cases.

Figure 4a shows an SEM top-view image of a Si-CHA layer that was coated on an $\alpha$-$Al_2O_3$ disk by the sonication-assisted deposition method. Most of the surface of the $\alpha$-$Al_2O_3$ disk seemed to be covered by platelike Si-CHA particles rather than conventional near-cubic particles. It was apparent that the deposited Si-CHA particles were closely packed with multiple layers to some extent. It appears that access of larger near-cubic particles to the disk surface was effectively limited by the clearance between the cover glass and the disk surface, and that this limited accessibility was beneficial in the selective coating of the $\alpha$-$Al_2O_3$ disk with the smaller platelike particles. Remarkably, even relatively small near-cubic particles (ca. 1–2 µm) were not deposited either on the $\alpha$-$Al_2O_3$ disk or on already-deposited platelike particles. Furthermore, physical interactions between the platelike Si-CHA particles and the $\alpha$-$Al_2O_3$ disk were sufficient for the formation of a uniform layer. Therefore, there was no need for any chemical attachment between the zeolite particles and the support, in contrast to the sonication-assisted chemical deposition method described previously.[34,35] Additional SEM images taken at two different sites and different magnifications are shown in Figure S4. It is possible that a uniform Si-CHA layer with a similar or higher degree of out-of-plane orientation or surface coverage could be formed by the sonication-assisted chemical deposition method described in the literature.[34,35] However, subsequent calcination, which is supposed to burn off any chemical linkers and promote the condensation of hydroxy groups between zeolite particles and the substrate, made no difference to chemically and physically deposited Si-CHA zeolite particles owing to the sufficient uniformity of the Si-CHA layer. Indeed, the avoidance of a complicated process involving surface functionalization by chemical linkers

makes the current approach attractive: control of the accessibility of the substrate to Si-CHA particles suffices for the formation of a uniform Si-CHA layer (Figure 4a).

Figure 4a shows that the platelike particles were deposited with the large plane parallel to the $Al_2O_3$ disk and thus possibly with an out-of-plane orientation. The corresponding XRD pattern (Figure 4b) confirms that the Si-CHA coating layer was oriented with the *h0h* plane perpendicular to the out-of-plane direction. For convenience, the out-of-plane orientation of the Si-CHA layer shown in Figure 4a is referred to as the *h0h* out-of-plane orientation. SEM and XRD analysis demonstrated that the basal plane in the platelike Si-CHA particles was the (101) plane and was equivalent to the face of the near-cubic Si-CHA particles shown in Figure 1. Furthermore, the interplanar angle[36] between the plane normal to the [211] zone axis (see Figure S2c) and the (101) plane was about 6.1°, which supports the hypothesis that the basal plane of platelike particles deposited nearly parallel to the surface of the α-$Al_2O_3$ disk, as shown in Figure 4a, was the (101) plane. The SAED pattern of a platelike particle was equivalent to that of a near-cubic particle (see Figures S2 and S3). This result indicates that the large basal plane in the platelike particles can be considered, geometrically speaking, as a slice of a near-cubic Si-CHA particle. Although additional investigations focused primarily on the early stages of CHA crystal growth are required, the observation of platelike Si-CHA particles might indicate a possible growth mechanism involving the stacking of their basal planes to eventually form near-cubic Si-CHA particles, as lamellar structures in near-cubic morphologies were reported for willhendersonite (isostructural to CHA zeolites)[37] and SAPO-34 (obtained by the transformation of lamellar AlPO-kanemite).[38]

Since 8-MR channels $(0.370 \times 0.417 \text{ nm}^2)$ run through both *a* and *b* axes, the 8-MR channels in the direction perpendicular to the *h0h* plane are tilted by about 47° with respect to the *a* or *b* axis. Accordingly, the tortuosity (defined in this case as the ratio of the actual path length across a film to the film thickness) across an *h0h*-oriented CHA film, if epitaxially well-grown from the uniform *h0h*-oriented Si-CHA layer in the current study, will be about 1.5 with respect to that of either the *a*- or *b*-oriented counterpart (i.e., equal to the secant of 47°). We further calculated the crystallographic preferential orientation (CPO) index to quantify the preferred out-of-plane orientation. The $CPO_{(101)/(2\bar{1}0)}$ index calculated from three different samples was approximately $24 \pm 8$, which indicates the pronounced alignment of the *h0h* plane in the out-of-plane direction.

Since the deposits possibly contained amorphous flakes, as indicated by the XRD pattern in Figure S1b, we further attempted the intergrowth of the layer in Figure 4a under synthetic conditions that lead to SSZ-13 zeolites (CHA-type zeolites).[39] Top-view and cross-sectional SEM images (see Figure S5) revealed that despite the possible presence of amorphous constituents, the secondary growth of the compact seed layer resulted in an approximately 1.5–2 μm thick, continuous CHA film. However, the *h0h* out-of-plane orientation in the seed layer was not well preserved during secondary growth (see Figure S5). Thus, additional studies are needed to trace the evolution of the out-of-plane orientation with the film thickness and provide an understanding of the growth behavior of CHA films.

In summary, we could selectively deposit platelike Si-CHA particles, although present in lower abundance in a mixture with near-cubic Si-CHA particles, on a porous α-$Al_2O_3$ disk to form a uniform *h0h*-out-of-plane-oriented Si-CHA layer. The successful formation of this layer was attributed to two main factors: 1) sonication enabled dispersed Si-CHA particles to reach the surface of the α-$Al_2O_3$ disk and physically deposit on it to form a continuous layer, and 2) cover glasses sandwiching the $Al_2O_3$ disk permitted only smaller platelike Si-CHA particles to reach the surface and prevented access to the more abundant and larger near-cubic particles. The control of accessibility enabled the depositing of thinner particles while excluding thicker particles. Such discrimination is otherwise quite challenging owing to the difficulty in separating mixed solids with different morphologies and sizes. An approximately 1 μm thick Si-CHA zeolite film on a tubular support (e.g., 1 cm in diameter and 10 cm in length) would correspond to a gain in weight of about 5 mg, indicating that only a small quantity of particles is sufficient to cover the entire surface area. Thus, our sonication-assisted deposition method can be regarded as an effective tool for the formation of a uniform layer, even when the desired particles exist as a minor fraction of a mixture. The *h0h*-oriented layer is a good candidate for use in the manufacture of oriented films through subsequent epitaxial secondary growth. Efforts to synthesize *h0h*-oriented continuous CHA films are under way.

### Experimental Section

[1] J. Kärger, D. M. Ruthven, *Diffusion in Zeolites and Other Microporous Solids*, Wiley, New York, **1992**.

[2] D. W. Breck, *Zeolite Molecular Sieves: Structure, Chemistry, and Use*, Wiley, New York, **1974**.

[3] N. Y. Chen, T. F. D. Degnan, Jr., S. C. Morris, *Molecular Transport and Reaction in Zeolites: Design and Application of Shape Selective Catalysts*, VCH, New York, **1994**.

[4] J. Weitkamp, L. Puppe, *Catalysis and Zeolites: Fundamentals and Applications*, Springer, Berlin, **1999**.

[5] J. Choi, H. K. Jeong, M. A. Snyder, J. A. Stoeger, R. I. Masel, M. Tsapatsis, *Science* **2009**, *325*, 590–593.

[6] K. Varoon, X. Y. Zhang, B. Elyassi, D. D. Brewer, M. Gettel, S. Kumar, J. A. Lee, S. Maheshwari, A. Mittal, C. Y. Sung, M. Cococcioni, L. F. Francis, A. V. McCormick, K. A. Mkhoyan, M. Tsapatsis, *Science* **2011**, *334*, 72–75.

[7] J. Caro, M. Noack, *Microporous Mesoporous Mater.* **2008**, *115*, 215–233.

[8] M. E. Davis, *Nature* **2002**, *417*, 813–821.

[9] E. E. McLeary, J. C. Jansen, F. Kapteijn, *Microporous Mesoporous Mater.* **2006**, *90*, 198–220.

[10] Y. S. Lin, I. Kumakiri, B. N. Nair, H. Alsyouri, *Sep. Purif. Methods* **2002**, *31*, 229–379.

[11] H. M. Kvamsdal, K. Jordal, O. Bolland, *Energy* **2007**, *32*, 10–24.

[12] K. Zenz House, C. F. Harvey, M. J. Aziz, D. P. Schrag, *Energy Environ. Sci.* **2009**, *2*, 193–205.

[13] T. C. Merkel, H. Q. Lin, X. T. Wei, R. Baker, *J. Membr. Sci.* **2010**, *359*, 126–139.

[14] D. Britt, H. Furukawa, B. Wang, T. G. Glover, O. M. Yaghi, *Proc. Natl. Acad. Sci. USA* **2009**, *106*, 20637–20640.

[15] W. J. Koros, R. Mahajan, *J. Membr. Sci.* **2000**, *175*, 181–196.

[16] S. G. Li, J. L. Falconer, R. D. Noble, *Adv. Mater.* **2006**, *18*, 2601–2603.

[17] M. Kanezashi, J. O'Brien-Abraham, Y. S. Lin, K. Suzuki, *AIChE J.* **2008**, *54*, 1478–1486.

[18] T. Tomita, K. Nakayama, H. Sakai, *Microporous Mesoporous Mater.* **2004**, *68*, 71–75.

[19] S. R. Venna, M. A. Carreon, *Langmuir* **2011**, *27*, 2888–2894.

[20] M. A. Carreon, S. G. Li, J. L. Falconer, R. D. Noble, *J. Am. Chem. Soc.* **2008**, *130*, 5412–5413.

[21] Y. Cui, H. Kita, K. Okamoto, *J. Mater. Chem.* **2004**, *14*, 924–932.

[22] J. van den Bergh, W. Zhu, J. Gascon, J. A. Moulijn, F. Kapteijn, *J. Membr. Sci.* **2008**, *316*, 35–45.

[23] Y. Y. Tian, L. L. Fan, Z. Y. Wang, S. L. Qiu, G. S. Zhu, *J. Mater. Chem.* **2009**, *19*, 7698–7703.

[24] N. Hedin, G. J. DeMartin, W. J. Roth, K. G. Strohmaier, S. C. Reyes, *Microporous Mesoporous Mater.* **2008**, *109*, 327–334.

[25] M. A. Snyder, M. Tsapatsis, *Angew. Chem.* **2007**, *119*, 7704–7717; *Angew. Chem. Int. Ed.* **2007**, *46*, 7560–7573.

[26] H. Y. Jiang, B. Q. Zhang, Y. S. Lin, Y. D. Li, *Chin. Sci. Bull.* **2004**, *49*, 2547–2554.

[27] Z. Lai, G. Bonilla, I. Diaz, J. G. Nery, K. Sujaoti, M. A. Amat, E. Kokkoli, O. Terasaki, R. W. Thompson, M. Tsapatsis, D. G. Vlachos, *Science* **2003**, *300*, 456–460.

[28] M. J. Díaz-Cabanas, P. A. Barrett, M. A. Camblor, *Chem. Commun.* **1998**, 1881–1882.

[29] J. Choi, S. Ghosh, Z. P. Lai, M. Tsapatsis, *Angew. Chem.* **2006**, *118*, 1172–1176; *Angew. Chem. Int. Ed.* **2006**, *45*, 1154–1158.

[30] E. A. Eilertsen, B. Arstad, S. Svelle, K. P. Lillerud, *Microporous Mesoporous Mater.* **2012**, *153*, 94–99.

[31] M. Trzpit, S. Rigolet, J. L. Paillaud, C. Marichal, M. Soulard, J. Patarin, *J. Phys. Chem. B* **2008**, *112*, 7257–7266.

[32] D. H. Olson, M. A. Camblor, L. A. Villaescusa, G. H. Kuehl, *Microporous Mesoporous Mater.* **2004**, *67*, 27–33.

[33] L. A. Villaescusa, I. Bull, P. S. Wheatley, P. Lightfoot, R. E. Morris, *J. Mater. Chem.* **2003**, *13*, 1978–1982.

[34] J. S. Lee, K. Ha, Y. J. Lee, K. B. Yoon, *Adv. Mater.* **2005**, *17*, 837–841.

[35] K. B. Yoon, J. S. Lee, K. Ha, Y.-J. Lee, Y. Chang (Sogang University), WO 2006/001648 A1, **2006**.

[36] A. Kelly, K. M. Knowles, *Crystallography and Crystal Defects*, Wiley, Chichester, **2012**.

[37] D. R. Peacor, P. J. Dunn, W. B. Simmons, E. Tillmanns, R. X. Fischer, *Am. Mineral.* **1984**, *69*, 186–189.

[38] A. Albuquerque, S. Coluccia, L. Marchese, H. O. Pastore, *Stud. Surf. Sci. Catal.* **2004**, *154*, 966–970.

[39] H. Kalipcilar, T. C. Bowen, R. D. Noble, J. L. Falconer, *Chem. Mater.* **2002**, *14*, 3458–3464.